A Hybrid CMOS-Microfluidic Contact Imaging Microsystem

Ritu Raj Singh[a], Lian Leng[b], Axel Guenther[b] and Roman Genov[a]

[a]Department of Electrical and Computer Engineering, University of Toronto, Toronto, Canada
[b]Department of Mechanical and Industrial Engineering, University of Toronto, Toronto, Canada

ABSTRACT

A hybrid CMOS/microfluidic microsystem is presented. The microsystem integrates a soft polymer microfluidic network with a 64x128 pixel imager fabricated in a low-cost standard 0.35 micron CMOS technology. The multiple microfluidic channels facilitate in-situ photochemical reactions of analytes and their detection directly on the surface of the CMOS photosensor array. The proximity between the analyte and the photosensor enhances the microsystem sensitivity, thus requiring only microliter volumes of the sample. Circuit techniques such as pixel binning and a two transistor reset path are employed to improve the imager sensitivity. The integrated microsystem is validated in on-chip chemiluminescence detection of luminol for the two microfluidic network prototypes designed.

Keywords: contact imaging, CMOS, microfluidics, chemiluminescence, dark current, transistor-sharing pixel

1. INTRODUCTION

There is a fast growing need for low-cost, small form factor biochemical sensory systems for applications such as on-site medical, environmental and biothreat monitoring. Optical biochemical sensing techniques such as chemiluminescence and fluorescence are widely popular in these applications,[1].[2] Conventional imaging systems for optical biochemical sensing involve bulky magnifying optics with a photodetector array. The high cost and the lack of portability makes them unsuitable for on-site and point-of-care applications.

Contact imaging is a compact and low-cost imaging technique.[3] The object to be imaged is placed in close proximity to the photodetector array. As compared to conventional optical imaging, contact imaging does not require intermediary optics, resulting in a significant area and cost savings. Moreover, contact imaging improves the light collection efficiency with orders of magnitude improvement in sensitivity.[4] This is so because the distance between the photodetector and the luminous object being imaged is of the same order as the size of the object. These advantages make contact imaging attractive for on-site deployable, low-cost biosensors.

Placing a luminous object such as a biochemical-sensitive light emitting analyte onto an imaging surface requires a compatible, versatile, high-resolution, parallel-structured fluidic channel network capable of analyte delivery and removal. Low-cost soft lithography based microfluidic channels are attractive for such applications.

Recently, several research groups reported integration of a sensory array with microfluidics for applications in cell culture, flow-based cytometry and capacitance-based fluid detection,[5],[6].[7] They implement simple forms of microfluidic integration by either non-contact based sensing or low spatial resolution microfluidic fabrication. Non-contact based sensing where the analyte is not in contact with the sensor results in a lower sensitivity and higher crosstalk. Lower spatial resolution microfluidics does not fully utilize the intrinsic parallelism of a microfluidic network and a sensor array.

In optical sensing applications, a highly parallel microfluidic network requires a massively parallel photosensory array for high throughput sensing. Charge coupled devices (CCDs), owing to their intrinsic serial readout structure and higher cost are not ideally suited for such applications. CMOS devices with their parallel readout

Further author information: (Send correspondence to Dr. Roman Genov.)
Dr. Roman Genov : E-mail: roman@eecg.toronto.edu

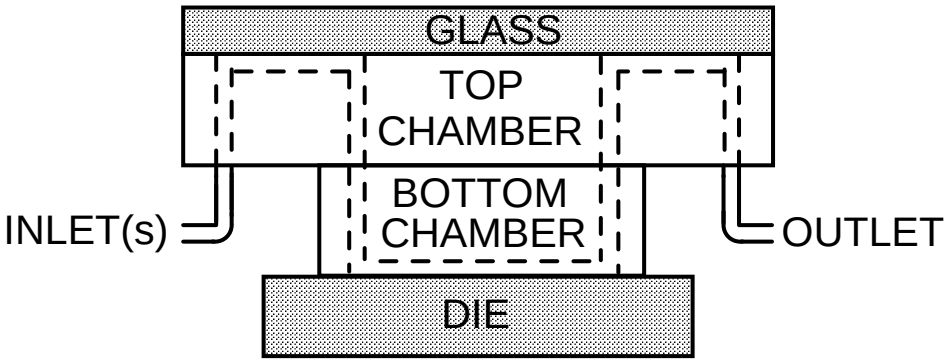

Figure 1. CMOS/microfluidic imager system diagram.

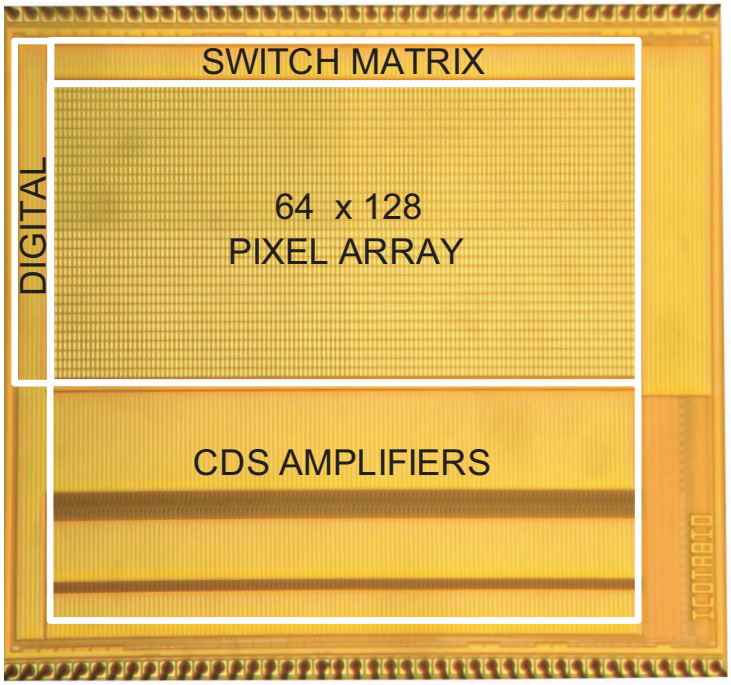

Figure 2. Chip micrograph.

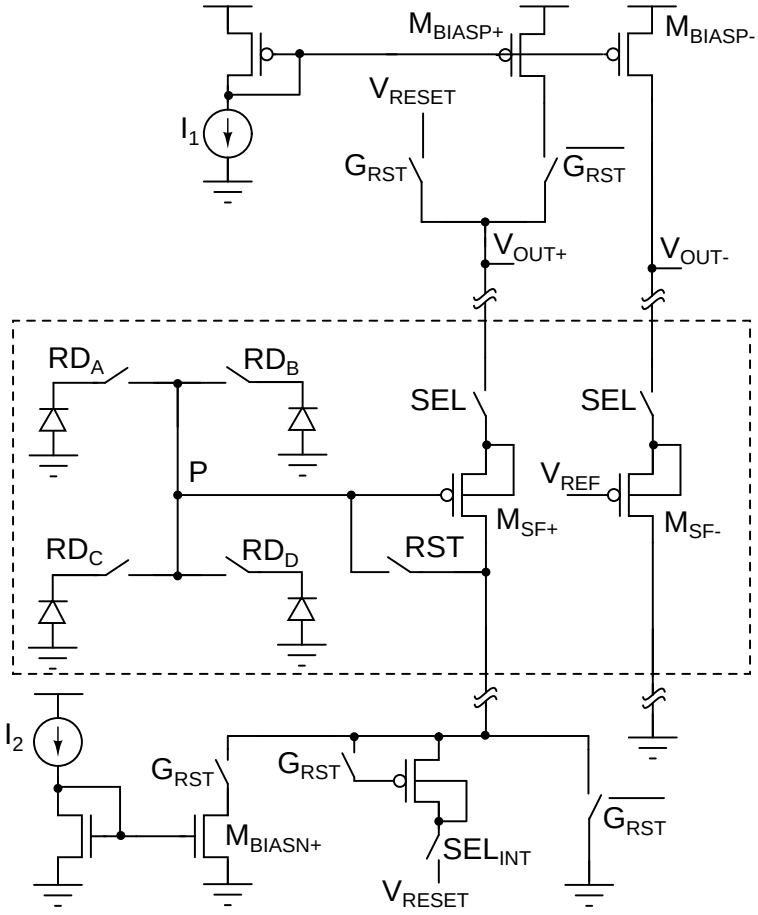

(a)

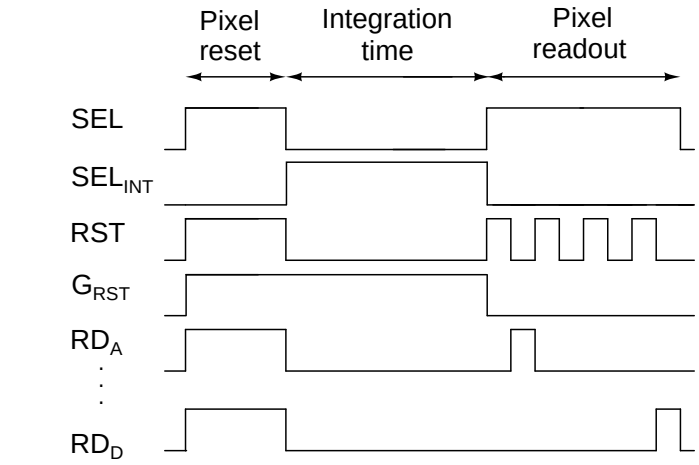

(b)

Figure 3. (a) Pixel and its column biasing circuit. (b) Timing diagram of the pixel.

structure and versatility of on-chip integration of signal conditioning circuits are an attractive choice for low-cost, high-throughput sensory microsystem implementation.

To further improve the detection limit of the resulting contact-based imaging system, the CMOS imager should be optimised for low-level light sensitivity. A two transistor reset path for resetting the photodiode has been proposed to reduce the subthreshold leakage component of the pixel dark current. An active reset technique[8] and differential signalling[9] have been employed to reduce the reset noise and supply noise respectively. Imaging high spatial resolution microfluidics requires fine spatial resolution pixel array. Unlike low spatial resolution photodetector arrays,[9] high photon collection efficiencies are difficult to obtain for small pixel sizes. A transistor sharing architecture has been utilized to increase the pixel fill factor,[10] hence improving sensitivity. Pixel binning has been employed to yield higher resolution images at no additional area penalty.[10]

We present a CMOS/microfluidic microsystem for direct-contact, high spatial resolution luminescence-based optical sensing of chemical analytes. We discuss the constituent parts of the assembly and provide experimental results validating the microsystem next.

2. MICROSYSTEM INTEGRATION

Figure 1 depicts the cross section of the proposed assembly of the microfluidic channel network over a CMOS chip to perform contact imaging. A two layer microfluidic structure is utilized. The top layer microfluidics contains the inlet and outlet interfaces for the fluidic network. The bottom layer microfluidics contains the fine spatial resolution microfluidic network which is routed over the CMOS sensory array. Routing the microfluidic channels over the CMOS chip results in an increased sensitivity and reduced crosstalk,[11].[4] The top layer and the bottom layer microfluidic channels are adhered to face against each other and to form channel networks with the glass layer and the CMOS die respectively. The entire microfluidic structure is compression sealed over the CMOS chip. The individual components of the microsystem assembly are discussed next.

3. CMOS IMAGER

Figure 2 shows the micrograph of the CMOS imager designed in a 0.35μm technology. It consists of a 128x64 pixel array, a bank of 128 column-parallel correlated double sampling amplifiers, and readout circuits. The size of a photodiode is 19μmx19μm and was chosen to be less than the Nyquist distance as dictated by the microfluidic channel width of 80μm.

A transistor sharing pixel architecture has been chosen.[12] Figure 3 shows the pixel circuit and its timing diagram. Sharing the source follower and the select transistor among the four photodiodes results in an increased pixel fill factor. The architecture also provides faster column readouts due to lower column capacitance and can perform in-pixel binning without any additional area cost.[10]

The four photodiodes sharing a single source follower can all be turned-on to form a single larger photodiode. This results in a higher signal-to-noise ratio for shot-noise limited scenarios. The imager shot-noise decreases with an increase in the photodiode capacitance.[13] Lumping the four photodiodes results in an increased capacitance. An n^+–p-substrate was chosen to implement the photodiode because it offered the highest capacitance density and has minimal layout constraints, resulting in a higher fill factor.

The total noise contribution of the select transistors in the transistor sharing architecture is minimal. They are minimum sized to reduce charge injection errors. A body-connected PMOS source follower minimizes the source follower nonlinearity.[9] Differential signaling reduces the effects of power supply fluctuations.[9] Due to relaxed temporal constraints in biochemical sensing applications, active reset technique is employed to reduce the reset noise of the photodiodes.[8]

Minimization of the photodiode dark current is crucial to facilitate large time of integration of the photocurrent, resulting in better sensitivity. Subthreshold leakage current from the adjoining transistor junctions can contribute significantly to the dark current.[14] The pixel architecture employs a two transistor reset path for resetting the photodiode through the *RST* and *RD* switch path. The subthreshold leakage current of a transistor is exponentially related to the drain source voltage applied across it. The distribution of the power supply-photodiode voltage drop between the *RST* and *RD* results in an exponential decrease in the subthreshold

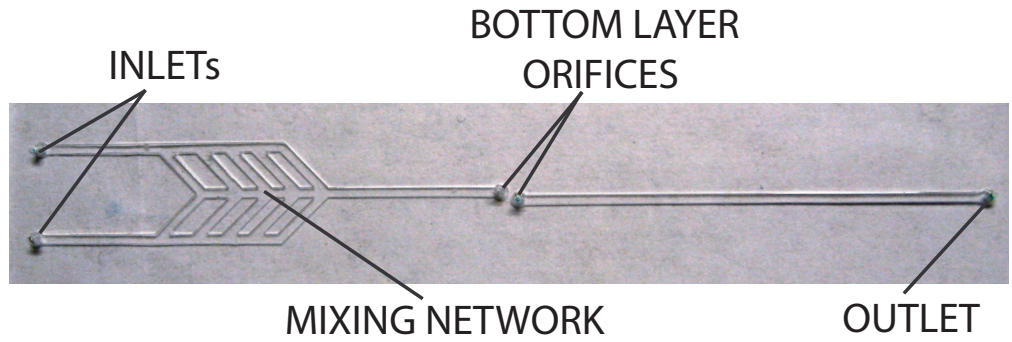

(a)

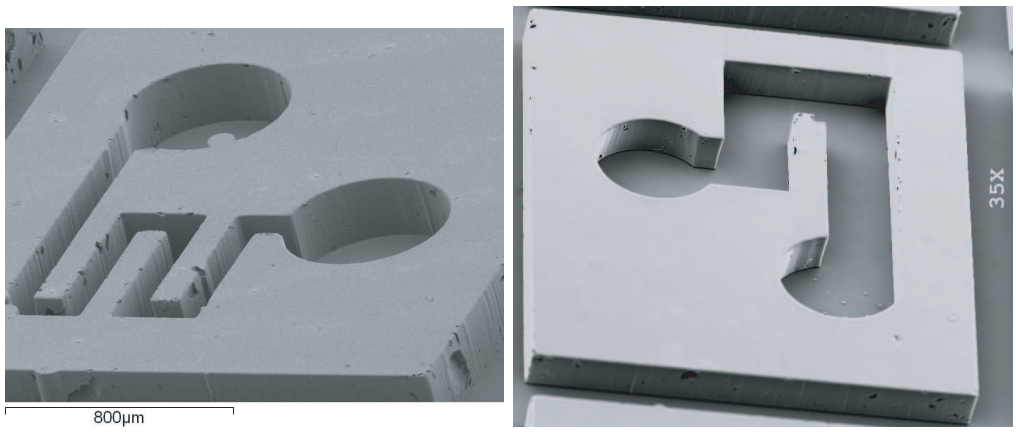

(b)

Figure 4. (a) Top layer microfluidic device. (b) SEM micrographs of two bottom layer microfluidic device samples.

leakage currents and hence its contribution to the photodiode dark current. A rectangular photodiode layout was used to minimize the dark current degradation due to edge effects.[15] To further reduce the peripheral dark current component, a polysilicon ring was placed at the edge of each photodiode to separate the defect prone periphery.[16]

A p^+ substrate ring surrounds the photodiodes to reduce on-chip crosstalk. A vertical metal-walled enclosure of the photodiodes reduces light crosstalk. The differential outputs from the photodiode array feed the column parallel amplifiers which perform correlated sampling of the pixel outputs.

3.1 Microfluidic Network

The on-chip microfluidic network consists of the top layer and the bottom layer. The top layer microfluidic device contains mixing channels for homogenous diffusion based mixing of the intake fluids. This enables in-situ chemical reactions for time-sensitive chemistries. The mixed fluids are then transported from the top layer to the bottom layer microfluidic network and over the CMOS sensory array. Due to the short distance between the site of reaction and sensory detection, the transient by-product, which is the emitted light in our case, can be easily detected by the photosensors.

Figure 4(a) shows a photograph of the one inch by three inch top layer microfluidic device. Figures 4(b) and (c) show SEM micrographs of two examples of the bottom layer microfluidic device. The depth of the channel in the top layer and the bottom layer devices is approximately 270μm. The channel width for the top layer and the bottom layer device are 300μm and 80μm respectively. The inlet and outlet on the bottom layer microfluidics measure 600μm in diameter and are placed such that they create a seal with the surface of the CMOS chip, outside of the active pixel array.

Table 1. SUMMARY OF IMAGER CHARACTERISTICS

Technology	0.35μm CMOS
Supply voltage	3.3V
Die area	2.9mm x 2.7mm
Array dimensions	64 x 128 pixels
Pixel size	19.0μm x 19.0μm
Fill factor	37%
Conversion gain	1.6 $\mu V/e^-$
Quantum efficiency @ 480nm	30%
Max. image SNR	54.4dB
Dark current	29 mV/sec
Operation rate	30 fps to 0.02fps
Max. integration time	1 min
Total power Pixel array power CDS power Digital power	29.3 mW 2.0mW 27.0mW 0.3 mW

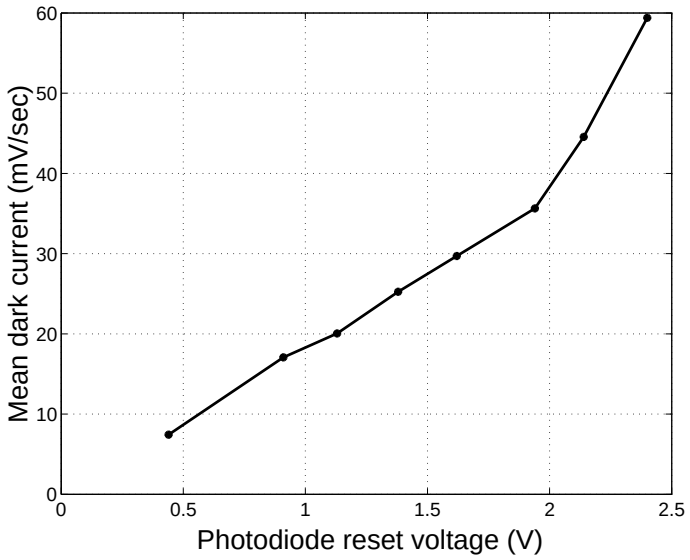

Figure 5. Experimentally measured photodiode dark current as a function of the reset voltage.

Soft lithography[17] was used to fabricate each layer of the microfluidic devices. A 1:10 ratio of curing agent and prepolymer polydimethylsiloxane (PDMS) was poured onto a master mold. The two master molds were fabricated by spincoating on cleaned glass slides two layers of negative photoresist SU8 2100 (MicroChem, MA) at 1750rpm, resulting in a total layer thickness of approximately 270μm. After soft baking the SU8 on hot plates at 65^{o}C and 95^{o}C, the designs were lithographically patterned onto the photoresist by UV exposing for 24.5 seconds through a transparency mask (CAD Art Services). The exposure time was determined for a Karl Suss MA6 with a 365nm lamp with intensity 15.5mW/cm^2 and a 405nm lamp with 31.0mW/cm^2 intensity. Upon molding, the two layers were treated in an oxygen plasma for 30 seconds and subsequently bonded. Hand pressed needles were used to puncture holes in the PDMS.

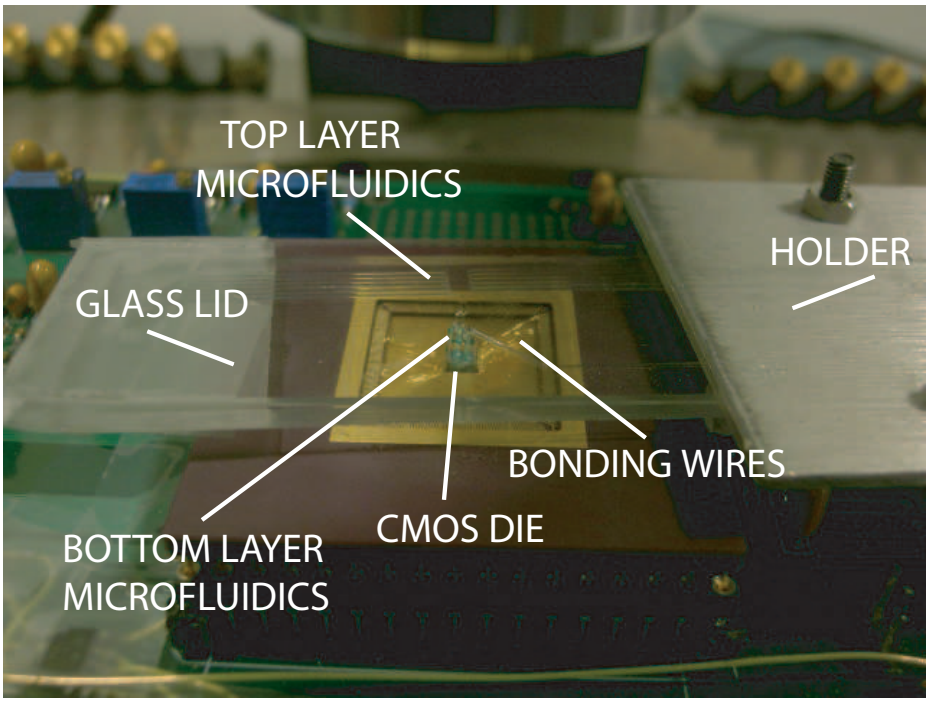

Figure 6. Closeup image of the microfluidic-imager assembly.

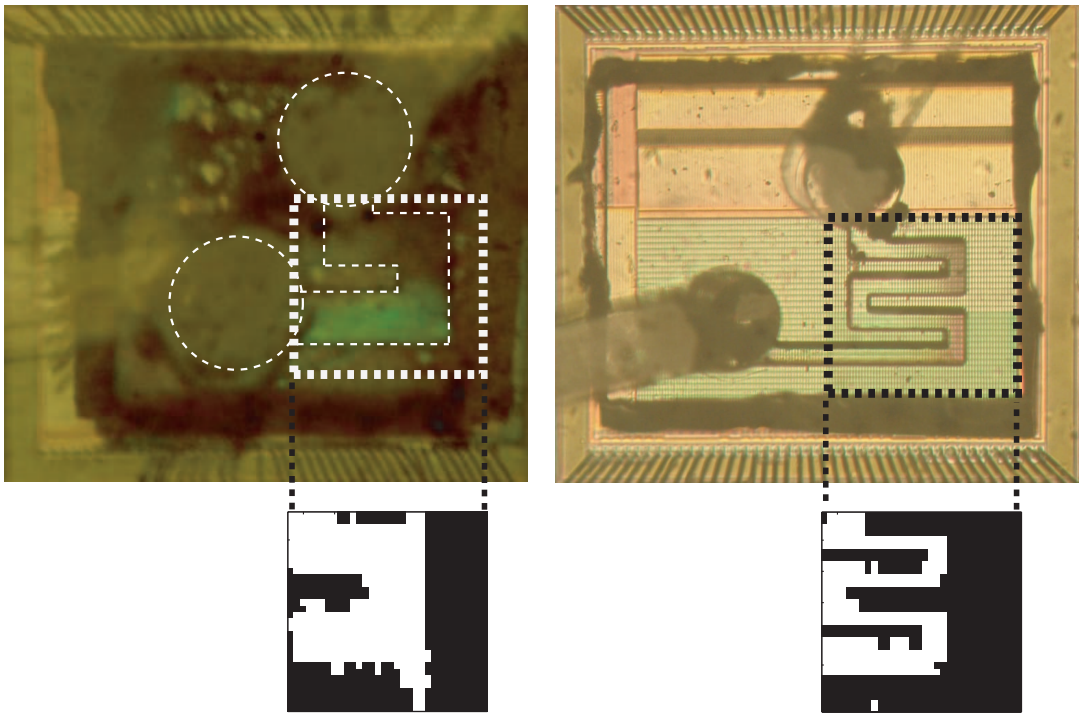

Figure 7. Experimentally captured luminol chemiluminescence (bottom) detected in the microfluidic channels placed over the CMOS die (top).

4. EXPERIMENTAL RESULTS

Table 1 summarizes the experimentally measured electrical characteristics of the image sensor chip. Figure 5 shows the experimentally recorded dark current with its corresponding reset voltage. The exponential dependence of the dark current suggests a significant presence of the exponentially-dependent depletion-region induced current while simultaneously validating the negligible presence of the subthreshold leakage current.

Figure 6 shows a snapshot of the microfluidic device placed over the CMOS chip. The handle is mounted on a micromanipulator which provides microscale precision alignment in X, Y, Z and Θ directions. The bottom layer microfluidic device is aligned over the CMOS die under a microscope. The microfluidic device is compression sealed against the CMOS die.

To validate functionality of the integrated microsystem and the low noise photosensitive circuits, a proof-of-concept on-chip chemiluminescence detection experiment was performed. Chemiluminescence based biochemical sensing is widely utilized. It is used to detect ions and chemicals in small concentrations that oxidise the luminescent chemical such as luminol to produce light. Light produced from the oxidation is detected by the imager.

In our experiment, luminol was diffusion mixed with hydrogen peroxide, a standard oxidising agent to produce chemiluminescent light. The two reactants, luminol and hydrogen peroxide, are fed using the two inlets on the top layer microfluidic structure. The reactants are mixed close to the inlet of the bottom layer microfluidic device. The short lived reaction produces light which is recorded when the mixture flows over the pixel array. The volume of the microfluidic channel over one pixel is approximately one microliter. The time of integration to collect sufficient amount of chemiluminescent light was set between 1 and 52 seconds. The microfluidic pattern was placed over one half of the pixel array. The pixel architecture was configured in the binning mode to provide a 32x32 pixel array resolution. Figures 7(top) shows the micrographs of the fluidic chambers of Figure 5(a) and (b) attached to the surface of the CMOS die. Figure 7(bottom) shows the experimentally recorded chemiluminescence detected over the chip, validating the microsystem assembly for biochemical detection.

5. CONCLUSION

A hybrid CMOS and microfluidic microsystem for optical contact imaging has been presented. It performs direct-contact imaging at a high spatial resolution, enabling the use of multiple microfluidic channels for a higher throughput. The microsystem has been experimentally validated in on-chip luminol chemiluminescence detection. The microsystem holds promise for the development of a low cost, small form factor, accurate chemical analyte sensing technology.

REFERENCES

1. L. J. Kricka and G. H. G. Thorpe, "Chemiluminescent and Bioluminescent Methods in Analytical Chemistry," *Analyst* **108**, pp. 1274–1296, Nov 1983.
2. O. S. Wolfbeis, *Fluorescence Methods and Applications*, Blackwell, 1st ed., 2008.
3. U. C. Fischer and H. P. Zingsheim, "Submicroscopic Contact Imaging with Visible Light by Energy Transfer," *Applied Physics Letters* **40**, pp. 195–197, Feb 1982.
4. K. Salama, H. Eltoukhy, A. Hassibi, and A. E. Gamal, "Modeling and Simulation of Luminescence Detection Platforms," *Biosensors and Bioelectronics* **19**, pp. 1377–1386, June 2004.
5. E. Ghafar-Zadeh and M. Sawan, "A core-CBCM sigma delta capacitive sensor array dedicated to lab-on-chip applications," *Sensors and Actuators A-Physical* **144**(2), pp. 304–313, 2008.
6. J. B. Christen and A. G. Andreou, "Design, Fabrication and Testing of a Hybrid CMOS/PDMS Microsystem for Cell Culture and Incubation," *IEEE Tran. on Biomedical Circuits and Systems* **1**, pp. 3–18, April 2001.
7. L. Hartley, K. V. I. S. Kaler, and O. Y. Pecht, "Hybrid Integration of an Active Pixel Sensor and Microfluidics for Cytometry on a Chip," *IEEE Tran. on Circuits and Systems* **54**, pp. 99–110, Jan 2007.
8. B. Fowler, M. Godfrey, J. Balicki, and J. Canfield, "Low-Noise Readout Using Active Reset for CMOS APS," in *Proceedings of SPIE*, **3965**, pp. 126–135, May 2000.

9. H. Elthoukhy, K. Salama, and A. Gamal, "A 0.18μm CMOS Bioluminescence Detection System-on-chip," *IEEE Journal of Solid-State Circuits* **41**, pp. 651–662, March 2006.
10. J. Choi, S. Han, S. Kim, S. Chang, and E. Yoon, "A Spatial-Temporal Multi-Resolution CMOS Image Sensor with Adaptive Frame Rates for Moving Objects in the Region-of-Interest," in *IEEE International Solid-State Circuits Conference*, pp. 502–503, Feb 2007.
11. H. Ji, D. Sander, A. Haas, and P. A. Abshire, "Contact Imaging: Simulation and Experiment," *IEEE Transactions on Circuits and Systems I: Regular Papers* **54**, pp. 1698–1710, August 2007.
12. M. Kasano, Y. Inaba, M. Mori, S. Kasuga, T. Murata, and T. Yamaguchi, "A 2.0-μm Pixel Pitch MOS Image Sensor With 1.5 Transistor/Pixel and an Amorphous Si Color Filter," *IEEE Tran. on Electron Devices* **53**, pp. 611–617, April 2006.
13. N. Faramarzpour, M. J. Deen, and S. Shirani, "An Approach to Improve the Signal-to-Noise Ratio of Active Pixel Sensor for Low-Light-Level Applications," *IEEE Tran. on Electron Devices* **53**, pp. 2384–2391, Sep 2006.
14. E. K. Bolton, G. S. Sayler, D. E. Nivens, J. M. Rochelle, S. Ripp, and M. L. Simpson, "Integrated CMOS Photodetectors and Signal Processing for Very Low-Level Chemical Sensing With the Bioluminescent Reporters," *Sensors and Actuators B* **85**, pp. 179–185, June 2002.
15. I. Shcherback, A. Belenky, and O. Yadid-Pecht, "Empirical Dark Current Modeling for Complementary Metal Oxide Semiconductor Active Pixel Sensor," *Optical Engineering* **41**, pp. 1216–1219, May 2002.
16. B. Choubey and S. Collins, "Low Dark Current Logarithmic Pixels," in *IEEE Midwest Symposium on Circuits and Systems*, pp. 376–379, Aug 2005.
17. Y. Xia and G. Whitesides, "Soft Lithography," *Annual Review of Material Science* **28**, pp. 153–184, 1998.